

Article

Surface Morphology at the Microscopic Scale, Swelling/Deswelling, and the Magnetic Properties of PNIPAM/CMC and PNIPAM/CMC/Fe₃O₄ Hydrogels

Marianna Uva ^{1,2} and Andrea Atrei ^{1,2,*}

¹ Dipartimento di Biotecnologie, Chimica e Farmacia, Università di Siena, Via A. Moro 2, 53100 Siena, Italy; marianna.uva@unisi.it

² CRISMA, Via. Matteotti 15 Colle di Val d'Elsa, 53034 Siena, Italy

* Correspondence: andrea.atrei@unisi.it; Tel.: +39-577-234371

Academic Editors: Dirk Kuckling and David Díaz Díaz

Received: 19 September 2016; Accepted: 5 December 2016; Published: 13 December 2016

Abstract: Poly(*N*-isopropylacrylamide) (PNIPAM) hydrogels containing carboxymethylcellulose (CMC) and CMC/Fe₃O₄ nanoparticles were prepared. Free-radical polymerization with BIS as cross-linker was used to synthesize the hydrogels. The morphology at the microscopic scale of these materials was investigated using field emission scanning electron microscopy (FESEM). The images show that CMC in the PNIPAM hydrogels induces the formation of a honeycomb structure. This surface morphology was not observed for pure PNIPAM hydrogels prepared under similar conditions. The equilibrium swelling degree of the PNIPAM/CMC hydrogels (5200%) is much larger than that of the pure PNIPAM hydrogels (2500%). The water retention of PNIPAM/CMC hydrogels above the volume phase transition temperature is strongly reduced compared to that of pure PNIPAM hydrogel. Both PNIPAM/Fe₃O₄ and PNIPAM/CMC/Fe₃O₄ hydrogels exhibit a superparamagnetic behavior, but the blocking temperature (104 K) of the former is higher than that of the latter (83 K).

Keywords: hydrogels; thermoresponsive materials; magnetic nanoparticles; poly(*N*-isopropylacrylamide) (PNIPAM); field emission scanning electron microscopy (FESEM)

1. Introduction

Poly(*N*-isopropylacrylamide) (PNIPAM) hydrogels are the most investigated thermoresponsive hydrogels [1]. Because of their capability to change volume reversibly at a transition temperature, hydrogels of PNIPAM or co-polymer of PNIPAM have applications in several fields ranging from drug delivery to environmental remediation [2,3]. The introduction of magnetic nanoparticles (NPs) into PNIPAM hydrogels allows to heat remotely the hydrogels by applying alternating magnetic fields of suitable frequencies [2]. In most of these applications the rate of the deswelling/swelling processes across the volume phase transition temperature (VPTT) is important [4]. Unfortunately, the response of macroscopic PNIPAM hydrogels to temperature changes is rather slow [5–7]. The collapse of the swollen hydrogel (with expulsion of water molecules out of the polymer matrix) has a complex dynamics involving diffusion of polymer segments and conformation changes of the polymer chains [8]. A contribution to slow the thermal response of PNIPAM hydrogels comes from the so-called “skin effect”, which is the formation of a dense, vitreous layer which prevents the exchange of water molecules between the hydrogel and the surrounding [9]. Several methods have been introduced to obtain PNIPAM hydrogels featuring a faster response to temperature variations. Some of these methods use the copolymerization of NIPAM with hydrophilic molecules to eliminate the skin effect and form hydrophilic channels for the diffusion of water molecules [9,10]. Other methods are based on promoting the formation of interconnected pores or use PNIPAM microgels embedded in

a macrogel [11,12]. It has been shown that the interpenetrating polymer network (IPN) or semi-IPN hydrogels of NIPAM with a hydrophilic polysaccharide such as sodium alginate have a faster response to temperature variation [13]. In the present work, we prepared PNIPAM hydrogels containing carboxymethylcellulose (CMC) and magnetite (Fe_3O_4) NPs coated with CMC. CMC, a hydrophilic, biocompatible derivative of cellulose, appears to be a suitable candidate to prepare PNIPAM hydrogels exhibiting a faster thermal response. The choice of CMC was also motivated by its ability to stabilize aqueous dispersions of magnetite NPs [14]. One of the aims of this study was to investigate the effect of CMC and CMC/ Fe_3O_4 NPs on the morphology at micrometric scale and on the swelling/deswelling properties of PNIPAM hydrogels. The other aim was to study the effect of coating magnetite NPs with CMC on the magnetic properties of PNIPAM hydrogels containing Fe_3O_4 NPs. The morphology of the PNIPAM hydrogels was investigated by means of field emission scanning electron microscopy (FESEM). The magnetic properties of PNIPAM/ Fe_3O_4 and PNIPAM/CMC/ Fe_3O_4 hydrogels were studied by measuring magnetization versus magnetic field curves at various temperatures, and zero field cooling (ZFC) and field cooling (FC) curves.

2. Results and Discussion

The attenuated total reflectance–Fourier transform infrared spectroscopy (ATR-FTIR) spectrum measured for the PNIPAM hydrogel containing 20 wt % of CMC (PNIPAM/CMC20) can be fitted by summing the spectra of PNIPAM dry hydrogel and CMC. The best fit is obtained by optimizing the weight factors of the intensities of the spectra of PNIPAM hydrogel and CMC (Figure 1). This result suggests that there are no large interactions between the PNIPAM network and the CMC chains which, otherwise, would produce variations of the peak positions and widths in the spectrum of PNIPAM/CMC hydrogel with respect to those of the pure components. Because of partial overlapping of the main peaks of PNIPAM and CMC and the relatively small contribution of CMC to the intensity of the PNIPAM/CMC20 spectrum, Fourier transform infrared spectroscopy (FTIR) is not able to reveal subtle changes in the spectrum, resulting from possible interactions between PNIPAM and CMC or cross-linking of CMC chains. Hence, attenuated total reflectance (ATR)-FTIR results are consistent with the formation of a semi-IPN, but the cross-linking of CMC chains, leading to a full IPN [15], cannot be ruled out.

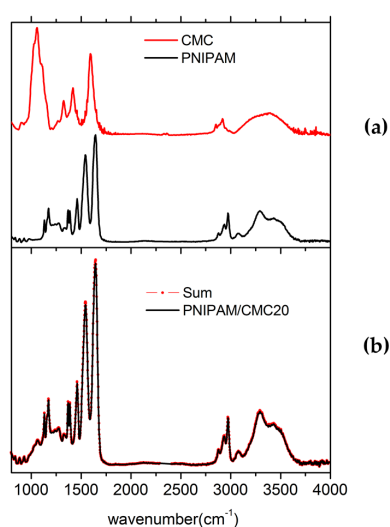


Figure 1. (a) Attenuated total reflectance–Fourier transform infrared spectroscopy (ATR-FTIR) spectra of carboxymethylcellulose (CMC) sodium salt and poly(*N*-isopropylacrylamide) (PNIPAM) hydrogel. The spectra were measured under the same instrumental conditions. (b) Fitting of the spectrum of the PNIPAM/CMC20 sample as a sum of the spectra of CMC and PNIPAM hydrogels weighted by optimized scaling factors. The spectra were measured for the lyophilized hydrogels.

FESEM images show that the microstructures of pure PNIPAM and PNIPAM/CMC lyophilized hydrogels are significantly different. Pure PNIPAM hydrogels have a morphology consisting of relatively flat foils over which large craters (size around 100 nm) are visible (Figure 2a). Even at higher magnifications, PNIPAM hydrogels exhibit a non-porous structure (Figure 2b). The images shown here are representative of the morphology of the whole samples.

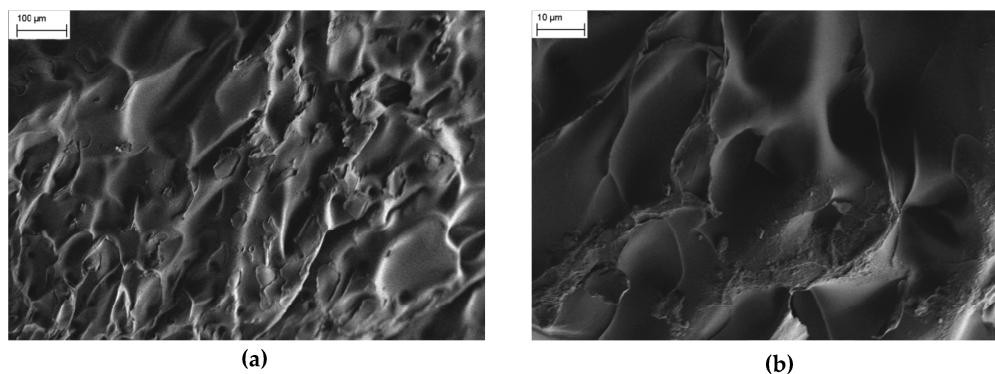


Figure 2. (a) Field emission scanning electron microscopy (FESEM) image collected for a pure PNIPAM hydrogels. (b) FESEM image collected for a pure PNIPAM hydrogel at a larger magnification.

On the other hand, FESEM images of PNIPAM/CMC are characterized by a honeycomb-like structure (Figure 3a,b), with features smaller than those observed in the images of pure PNIPAM. Images of internal cross sections of the PNIPAM/CMC hydrogels show that a network of interconnected pores exists inside the hydrogels. The observed honeycomb-like structure is probably due to the emergence of micropores at the surface of the PNIPAM/CMC hydrogels as suggested by the images measured for the inner cross-sections of the hydrogel (Figure 3c). The surface morphology of the PNIPAM/CMC hydrogels does not change significantly in the explored range of CMC concentration (that is from 5 wt % to 20 wt %) as far as the presence of pores is concerned. However, the size of the micropores tends to be smaller for the lower CMC concentration (Figure 3d).

The surface morphology of the hydrogels is not significantly affected by the presence of CMC/Fe₃O₄ NPs as shown by the FESEM images of the PNIPAM/CMC hydrogel containing 4.3 wt % magnetite (PNIPAM/CMC5/Fe₃O₄) samples (Figure 4a,b).

The attainment of the equilibrium swelling degree (SD_{eq}) was checked by measuring swelling kinetics starting from lyophilized samples of the hydrogels (Figure 5). These data indicate that the swelling process is slightly faster for the PNIPAM/CMC20 hydrogel than for the pure PNIPAM hydrogel. The SD_{eq} measured at 295 K of the PNIPAM/CMC20 sample ($5200\% \pm 200\%$) is much larger than that of the PNIPAM hydrogel ($2500\% \pm 200\%$). On the contrary, the addition of 5 wt % of CMC to the PNIPAM hydrogels slightly reduces its SD_{eq} ($1900\% \pm 100\%$). Similar SD_{eq} values (ca. 2000%) were measured for the PNIPAM/CMC5/Fe₃O₄ hydrogel. These results can be explained considering that the interactions of the hydrophilic groups of PNIPAM with those of CMC are more favorable than with water at low CMC concentration; thus, a decrease of the swelling degree is observed [15].

The VPTT estimated from the temperature at which the hydrogel samples start to be opalescent is not affected (within an uncertainty of ± 2 K) by CMC. This result was confirmed by the swelling degree measurements as a function of temperature of PNIPAM/CMC20 hydrogels which show a drastic change from 303 to 307 K. Moreover, the presence of CMC/Fe₃O₄, at the concentrations used in this work, does not influence, within the accuracy of the measurements, the VPTT of the PNIPAM hydrogels.

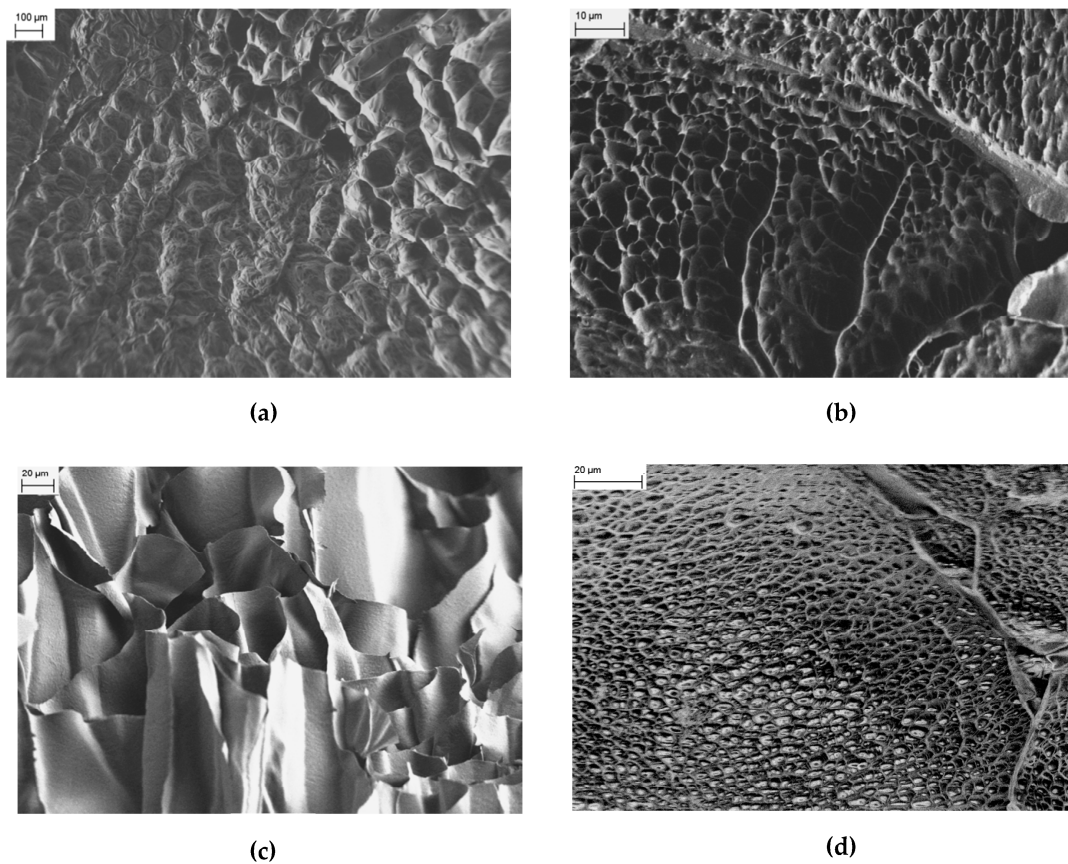


Figure 3. (a) FESEM image collected for a PNIPAM/CMC20 sample. (b) FESEM image collected for a PNIPAM/CMC20 sample at a larger magnification. (c) FESEM image of an inner cross section of the PNIPAM/CMC20 sample. (d) FESEM image of a PNIPAM hydrogel containing 5 wt % of CMC.

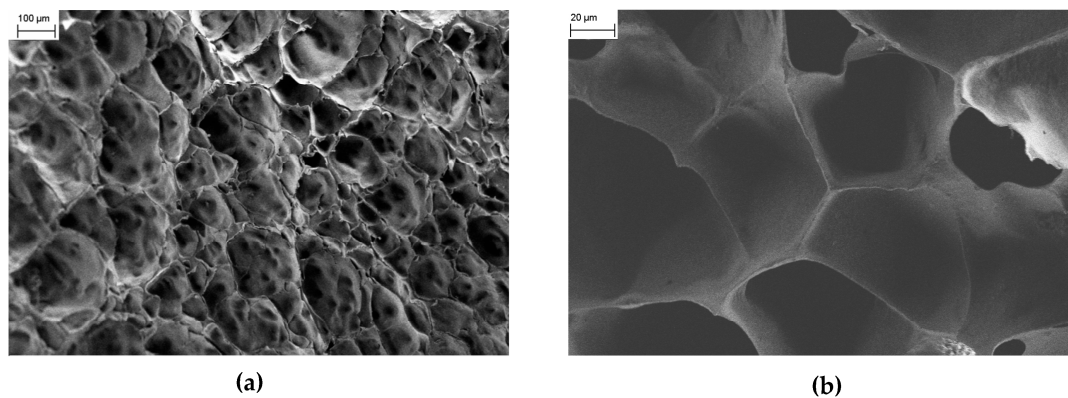


Figure 4. (a) FESEM image of the PNIPAM/CMC5/Fe₃O₄ hydrogel. (b) FESEM image collected for the PNIPAM/CMC5/Fe₃O₄ hydrogel at a larger magnification. FESEM image of a PNIPAM/CMC sample containing 5 wt % of CMC.

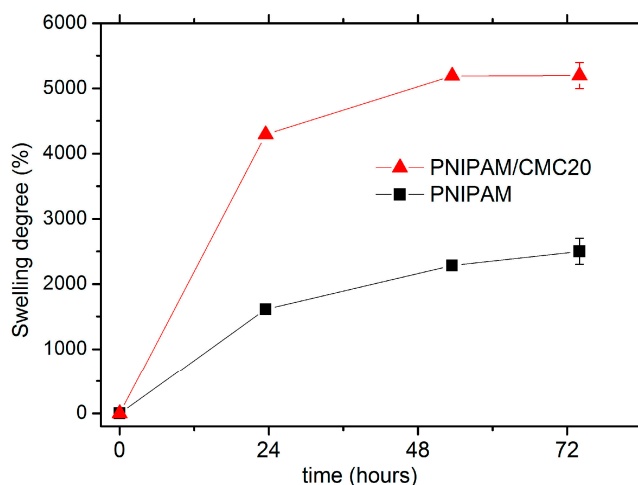


Figure 5. Swelling kinetics of PNIPAM and PNIPAM/CMC20 hydrogels in water at 295 K.

The deswelling kinetics of PNIPAM/CMC20 and of pure PNIPAM hydrogel samples, previously swollen in water at 295 K, were measured by monitoring the water retention % as a function of the immersion time in water at 313 K. After 30 min, the water retention of the PNIPAM/CMC20 hydrogel is reduced to about 35%, whereas that of pure the PNIPAM hydrogel reaches a steady-state value of 70% (Figure 6). Similar results were reported for PNIPAM/sodium alginate semi-IPNs [13]. The higher water retention of the pure PNIPAM hydrogel is due to the formation of a compact, vitreous layer at the surface of the samples above the VPTT, which hampers the release of water. The addition of CMC prevents the formation of this impermeable layer. This interpretation is supported by the different macroscopic morphology of the two kinds of hydrogels in water at 40 °C. The bubbles (full of water) that form at the surface of pure PNIPAM hydrogels in water above the VPTT [7] are not observed for the PNIPAM/CMC samples.

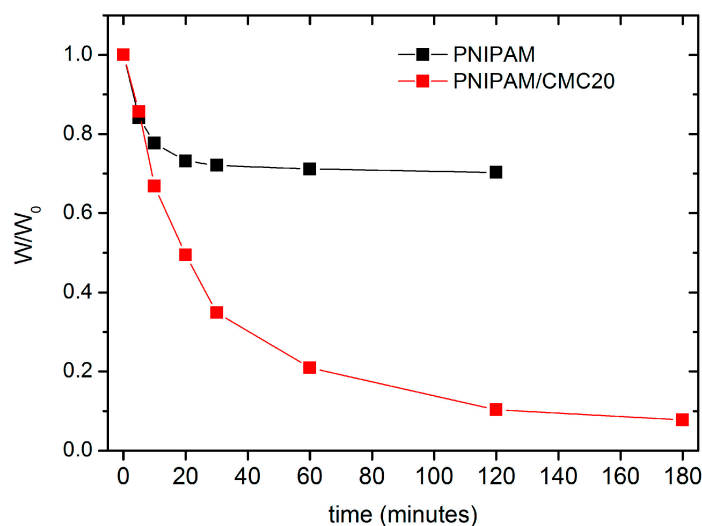


Figure 6. Water retention (defined as the weight W of the hydrogel divided by weight of the hydrogel swollen at 295 K W_0) as a function of immersion time in water at 315 K for the pure PNIPAM and the PNIPAM/CMC20 hydrogels.

Magnetization vs. magnetic field intensity curves were measured for PNIPAM/CMC5/Fe₃O₄ and PNIPAM/Fe₃O₄ hydrogels to investigate the effect of CMC on the magnetic properties of the hybrid organic–inorganic hydrogels. Magnetization vs. magnetic field intensity curves

of PNIPAM/CMC5/Fe₃O₄ and PNIPAM/Fe₃O₄ hydrogels show that the magnetic NPs are superparamagnetic. The magnetization vs. magnetic field intensity curves measured at 2.5 and 300 K for the PNIPAM/CMC5/Fe₃O₄ hydrogel are shown in Figure 7a. The curves measured at room temperature do not show any remanence. On the contrary, a hysteresis loop is observed in the curves measured at 2.5 K, with a remanent magnetization of 18 emu/g Fe₃O₄ and a coercive field of ca. 350 Oe (Figure 7a). The saturation magnetizations (63 and 52 emu/g Fe₃O₄ at 2.5 and 300 K, respectively) measured for the PNIPAM/CMC5/Fe₃O₄ hydrogel are higher than those of PNIPAM/Fe₃O₄ (46 and 33 emu/g Fe₃O₄ at 2.5 and 300 K, respectively). These values are lower than that of bulk magnetite (92 emu/g at room temperature) but comparable with those of magnetite NPs of similar size [16]. The ZF and ZFC curves confirm that magnetite NPs in the PNIPAM/CMC5/Fe₃O₄ hydrogel are superparamagnetic with a blocking temperature (T_b) of 83 K (Figure 7b). T_b measured for the PNIPAM/Fe₃O₄ hydrogel is 104 K, higher than that of the PNIPAM/CMC5/Fe₃O₄ hydrogel. Although many parameters can affect T_b (particle size, degree of oxidation, etc.), an increase in the number of particles in the clusters enhances the dipole–dipole interactions leading to an increase of T_b [16]. Hence, the observed difference of T_b suggests that the clusters of magnetite NPs are smaller in PNIPAM/CMC/Fe₃O₄ hydrogels than in PNIPAM/Fe₃O₄ hydrogels.

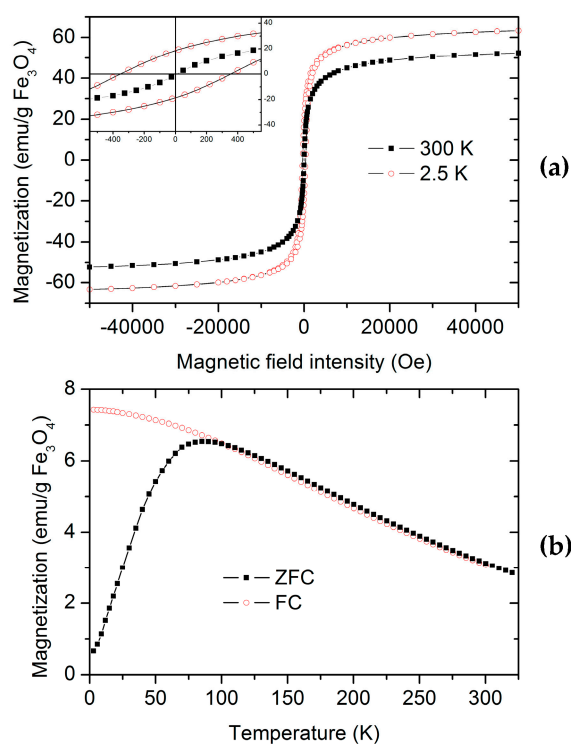


Figure 7. (a) Magnetization versus field intensity measured for the PNIPAM/CMC5/Fe₃O₄ lyophilized hydrogel at 2.5 K and 300 K. In the inset the curves at low intensity magnetic field are shown; (b) panel: zero field cooling (ZFC) and field cooling (FC) curves measured for the PNIPAM/CMC5/Fe₃O₄ sample. These curves were measured with an applied field of 50 Oe.

3. Conclusions

The surface morphology at micrometric scale of PNIPAM/CMC hydrogels is characterized by a porous network structure which is not observed for pure PNIPAM hydrogels. These features are probably the emergence of micropores at the surface of the material. With an equal cross-linking degree, PNIPAM hydrogels containing 20 wt % of CMC have a much larger equilibrium swelling degree than pure PNIPAM hydrogels. The observed reduction of water retention for the PNIPAM/CMC hydrogels above the VPTT compared to pure PNIPAM hydrogels can reasonably be attributed to their

surface morphology. The microporosity of the PNIPAM/CMC hydrogels prevents the formation of the dense layer impermeable to water as occurs for pure PNIPAM hydrogels. Moreover, the surface morphology of the PNIPAM/CMC5/Fe₃O₄ hydrogel is characterized by a honeycomb-like structure similar to PNIPAM/CMC hydrogels. Fe₃O₄ NPs prepared by co-precipitation in the presence of CMC embedded in PNIPAM hydrogels exhibit a superparamagnetic behavior. The lower blocking temperature measured for the PNIPAM/CMC5/Fe₃O₄ hydrogel compared to the PNIPAM/Fe₃O₄ hydrogel suggests that smaller aggregates of NPs are present in the PNIPAM/CMC5/Fe₃O₄ hydrogel. The capability of the PNIPAM/CMC hydrogels to absorb and release larger volumes of water at higher rates compared to pure PNIPAM hydrogels is important for many applications.

4. Materials and Methods

NIPAM, *N,N'*-methylenebisacrylamide (BIS), *N,N,N',N'*-tetramethylethylenediamine (TEMED), K₂S₂O₈, CMC sodium salt (molecular weight 700 kDa, 0.8 substitution degree), FeCl₃·6H₂O, and FeSO₄·(NH₄)₂SO₄·6H₂O were purchased from Sigma-Aldrich (St. Louis, MO, USA) and used as received. Deionized water was used for the experiments. PNIPAM hydrogels were prepared according to a free-radical polymerization procedure. The molar ratios of BIS, TEMED, and K₂S₂O₈ with respect to NIPAM were 2%, 10%, and 0.25%, respectively. For the preparation of PNIPAM/CMC hydrogels, the reaction was carried out in water solutions of CMC. Hydrogels containing 5 and 20 wt % CMC with respect to NIPAM are indicated as PNIPAM/CMC5 and PNIPAM/CMC20, respectively. Fe₃O₄ NPs were prepared by co-precipitation from Fe(II)/Fe(III) (1:2 stoichiometric ratio) solutions by adding NaOH in the presence of CMC at 333 K [14]. The size of the Fe₃O₄/CMC NPs was 9 ± 1 nm, as determined by X-ray diffraction in a previous work [14]. The composition of the CMC/magnetite dispersions was 50 wt %. The preparation of the PNIPAM hydrogels containing 5 wt % CMC and 5 wt % Fe₃O₄ (with respect to PNIPAM) was carried out in aqueous dispersions of CMC/Fe₃O₄ NPs. The PNIPAM sample with embedded Fe₃O₄ NPs was prepared by carrying out the PNIPAM hydrogel synthesis in a water dispersion of Fe₃O₄ NPs, previously prepared using the coprecipitation method. The concentrations of magnetite in the samples (as determined by UV-visible spectrophotometry [14]) was 4.3 ± 0.2 wt % and 1.5 ± 0.2 wt % (with respect to PNIPAM) for the PNIPAM/CMC/Fe₃O₄ and PNIPAM/Fe₃O₄ samples, respectively. These samples will be indicated as PNIPAM/CMC5/Fe₃O₄ and PNIPAM/Fe₃O₄. After prolonged washing in deionized water to remove unreacted species, the hydrogels were frozen and lyophilized.

The equilibrium swelling degree (SD_{eq}), defined as $(w - w_d)/w_d$ %, where w and w_d are the weights of the swollen and of the dried hydrogel, was measured in deionized water at 295 K. Attenuated total reflectance–Fourier transform infrared (ATR-FTIR) spectra were collected using a FTS6000 spectrometer (Bio-Rad, Cambridge, MA, USA) at a resolution of 4 cm⁻¹. A sigma VP FESEM microscope (Zeiss, Germany) was used for the FESEM measurements. The energy of the electron beam was in the range 1–10 keV, and the “in lens” detector was used to collect the secondary electrons. Measurements were performed under high vacuum conditions on the lyophilized samples without metallization or graphitization.

Magnetization versus field intensity and zero field cooling (ZFC) and field cooling (FC) curves were measured by means of a Superconducting Quantum Interference Device magnetometer (Quantum Design Ltd. San Diego, CA, USA).

Acknowledgments: This work was financially supported by MIUR (Ministero Istruzione Università e Ricerca) under the FIRB project RBAP11ZJFA, 2010. The authors are indebted to Claudia Innocenti (INSTM and Dipartimento di Chimica U. Schiff, Università di Firenze) for the magnetic measurements.

Author Contributions: Both authors conceived, designed, and performed the experiments. Both authors revised, read, and approved the final manuscript.

Conflicts of Interest: The authors declare no conflict of interest.

References

1. Nguyen, H.H.; Payre, B.; Fitremann, J.; Lauth-de Viguerie, N.; Marty, J. Thermoresponsive Properties of PNIPAM-Based Hydrogels: Effect of Molecular Architecture and Embedded Gold Nanoparticles. *Langmuir* **2015**, *31*, 4761–4768. [[CrossRef](#)] [[PubMed](#)]
2. Satarkar, N.S.; Hilt, J.Z. Magnetic hydrogel nanocomposite for remote controlled pulsative drug release. *J. Control. Release* **2008**, *130*, 246–251. [[CrossRef](#)] [[PubMed](#)]
3. Jing, G.; Wang, L.; Yu, H.; Amer, W.A.; Zhang, L. Recent progress on study of hybrid hydrogels for water treatment. *Colloids Surf. A* **2015**, *416*, 86–94. [[CrossRef](#)]
4. Imaran, A.B.; Seki, T.; Takeoka, Y. Recent advances in hydrogels in terms of fast stimuli responsiveness and superior mechanical performance. *Polym. J.* **2010**, *42*, 839–851. [[CrossRef](#)]
5. Depa, K.; Strachota, A.; Slouf, M.; Hromadkova, J. Fast temperature-responsive nanocomposite PNIPAM hydrogels with controlled pore wall thickness: Force and rate of T-response. *Eur. Polym. J.* **2012**, *48*, 1997–2007. [[CrossRef](#)]
6. Hirose, H.; Shibayama, M. Kinetics of Volume Phase Transition in Poly(*N*-isopropylacrylamide-co-acrylic acid) Gels. *Macromolecules* **1998**, *31*, 5336–5342. [[CrossRef](#)]
7. Shibayama, M.; Nagai, K. Shrinking Kinetics of Poly(*N*-isopropylacrylamide) Gels T-jumped across Their Volume Phase Transition Temperature. *Macromolecules* **1999**, *32*, 7461–7468. [[CrossRef](#)]
8. Sun, S.; Hu, J.; Tang, H.; Wu, P. Chain Collapse and Revival Thermodynamics of Poly(*N*-isopropylacrylamide) Hydrogel. *J. Phys. Chem. B* **2010**, *114*, 9761–9770. [[CrossRef](#)] [[PubMed](#)]
9. Kaneko, Y.; Nakamura, S.; Kiyotaka, S.; Aoyagi, T.; Kikuchi, A.; Sakurai, Y.; Okano, T. Rapid Deswelling Response of Poly(*N*-isopropylacrylamide) Hydrogels by the Formation of Water Release Channels Using Poly(ethylene oxide) Graft Chains. *Macromolecules* **1998**, *31*, 6099–6105. [[CrossRef](#)]
10. Gil, E.S.; Hudson, S.M. Effect of Silk Fibroin Interpenetrating Networks on Swelling/Deswelling Kinetics and Rheological Properties of Poly(*N*-isopropylacrylamide) Hydrogels. *Biomacromolecules* **2007**, *8*, 258–264. [[CrossRef](#)] [[PubMed](#)]
11. Zhao, Z.X.; Li, Z.; Xia, Q.B.; Bajalis, E.; Xi, H.X.; Lin, Y.S. Swelling/deswelling kinetics of PNIPAAm hydrogels synthesized by microwave irradiation. *Chem. Eng. J.* **2008**, *142*, 263–270. [[CrossRef](#)]
12. Xia, L.; Xie, R.; Ju, X.; Wang, Q.; Chen, Q.; Chu, L. Nano-structured smart hydrogels with rapid response and high elasticity. *Nat. Commun.* **2013**, *4*, 2226. [[CrossRef](#)] [[PubMed](#)]
13. Zhang, G.; Zha, L.; Zhou, M.; Ma, M.; Liang, B. Rapid deswelling of sodium alginate/poly(*N*-isopropylacrylamide) semi-interpenetrating polymer network hydrogels in response to temperature and pH changes. *Colloid Polym. Sci.* **2005**, *283*, 431–438. [[CrossRef](#)]
14. Maccarini, M.; Atrei, A.; Innocenti, C.; Barbucci, R. Interactions at the CMC/magnetite interface: Implications for the stability of aqueous dispersions and magnetic properties of magnetite nanoparticles. *Colloids Surf. A* **2014**, *462*, 107–114. [[CrossRef](#)]
15. Ekici, S. Intelligent poly(*N*-isopropylacrylamide)-carboxymethyl cellulose full interpenetrating polymer networks for protein adsorption studies. *J. Mater. Sci.* **2011**, *46*, 2843–2850. [[CrossRef](#)]
16. Mandel, K.; Hutter, F.; Gellermann, C.; Sextl, G. Stabilisation effects of superparamagnetic nanoparticles on clustering in nanocomposite microparticles and on magnetic behavior. *J. Magn. Magn. Mater.* **2013**, *331*, 269–275. [[CrossRef](#)]

